

Processing for Improved Spectral Analysis

Eric Bechhoefer¹, Brandon Van Hecke² and David He²

¹Green Power Monitoring Systems, LLC, Vermont, 05753, USA
eric@gpms-vt.com¹

²Dept of Mechanical and Industrial Engineering, The University of Illinois at Chicago, Illinois, 60607 USA
bvanhe2@uic.edu²
davidhe@uic.edu²

ABSTRACT

The Fast Fourier Transform (FFT) is the workhorse of condition monitoring analysis. The FFTs' assumption of stationarity is often violated in rotating machinery. Even in a six second acquisition on a wind turbine, the shaft speed can change by 5%. For Shaft and Gear analysis, this is mitigated through the use of the time synchronous average. For general spectrum analysis, or bearing envelope analysis, there is no such mitigation: one hopes that the effect of variation in shaft speed is small. Presented is a time synchronous resampling algorithm which corrects for variation in shaft speed, preserving the assumption of stationarity. This allows for improved spectral analysis, such as used in bearing fault detection. This is demonstrated on a real world-bearing fault.

1. INTRODUCTION

It would be hard to imagine the condition monitoring (CM) of rotating equipment without the use of the Fast Fourier Transform (FFT). Everything from simple spectrums (such as Welch's method for power spectral density), to more advanced analysis (amplitude modulation and frequency modulation analysis (McFadden, 1985)) are dependent on the FFT.

In using the FFT, the CM practitioner must understand the base assumptions of continually differentiable (Gibbs Effect), and stationarity. In general, window functions (Hann, Hamming, etc.) are used to control or mitigate Gibbs effect, while the time synchronous average (TSA, McFadden 1987, Bechhoefer, 2009a), is used to mitigate the effect of non-stationarity in rotating machinery for shaft and gear analysis.

The issue of non-stationarity is not well addressed for the

power spectral density (such as Welch's method), or for bearing analysis (envelope/heterodyne methods included). It is assumed that the smearing of energy due to changing shaft speed is small. For bearing analysis, the energy associated with a fault frequency is trended. A poor measure of that energy will result in variance in the trend, or just an inaccurate estimate of component damage.

Variance in shaft speed in rotating equipment is always present to varying degrees. The variation is due to:

- Limits in the control system bandwidth,
- Varying loads associated with the work the machine is producing,
- Or in the case of wind turbines, varying wind speed and torque ripple

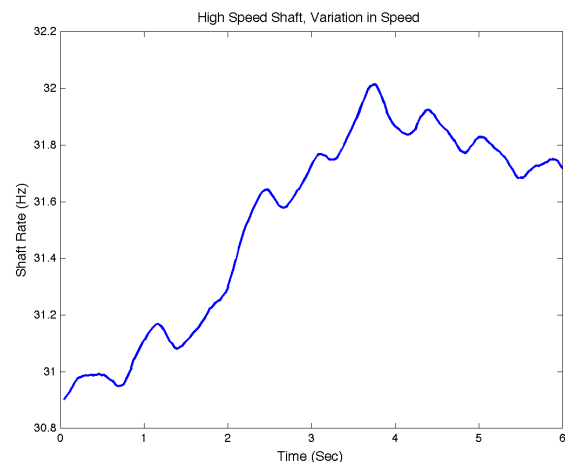


Figure 1. Variation in High Speed Shaft over 6 Second Acquisition

Wind turbines pose a particularly difficult environment. The wind, as noted, is time varying. Additionally, because the flow of wind is stalled in front of the tower, the lift on a blade as it passes in front the tower is reduced. This causes a 3/revolution torque ripple/change in shaft rate (Figure 1).

Bechhoefer, E. et al. This is an open-access article distributed under the terms of the Creative Commons Attribution 3.0 United States License, which permits unrestricted use, distribution, and reproduction in any medium, provided the original author and source are credited.

Finally, because of wind shear, the wind speed at the top of the rotor arc is greater than the bottom of the arc. Figure 1 shows the variance of a high-speed shaft on a wind turbine, over a 6 second acquisition. The instantaneous speed of the shaft is seen to range from 30.9 Hz to a maximum of 32.01 Hz, or a change in speed of 3.6%.

Consider the effect of this variation in speed on the spectral content of a bearing fault frequency, where the cage, ball, inner and outer race rates are: [0.42, 2.87, 9.46, 6.72]. The range of fault frequencies (Hz) during this acquisition are:

Table 1. Bearing Rates

Bearing\shaft	Low: 30.9	High 32.01
Cage (Hz)	12.98	13.44
Ball (Hz)	88.69	91.88
Inner Race (Hz)	292.3	302.8
Outer Race (Hz)	207.7	215.1

For the higher frequency bearing components, (inner/outer race), the frequency difference is significant: approximately 10 Hz. For spectral analysis, it poses a problem. Not only is there the issue of the spectral content smeared across a number of bins, but also which shaft rate does one use for analysis (the mean shaft rate over the acquisition)?

This issue of spectral spreading in the FFT is not academic. Consider the trend of an inner race fault on a high-speed shaft (Figure 2). The variance in the condition indicator is proportional to the inner race energy. While vibration measurements are stochastic, not all of the variation in Figure 2 is due to measurement noise. We will show that some portion of the condition indicator (CI) is a function measurement error due to variance in shaft speed.

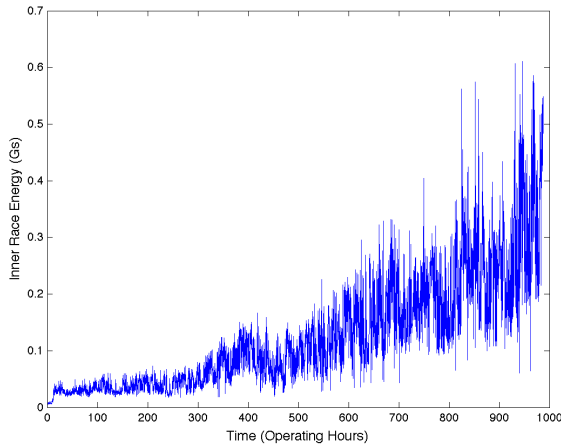


Figure 2. Trend of an inner race fault

This increased variance affects both the threshold setting process and alerting. Clearly if one does not have the luxury of sampling under steady state, a process is needed to mitigate the change in shaft RPM. We will show that

resampling is one method that can be used to reduce the variance in the measured bearing energy.

1.1. Units of Measurement

In this paper, the units are in G's, where 1g is the earth standard gravitational acceleration. While the sensors output voltage, the accelerometer manufacture defines the scale value to convert for volts to G's. The ISO (ISO 10816) has developed standards for vibration limits for rotating industrial machinery, these standards are limited for equipment running between 10-200 Hz. Additionally, the limits are directed at imbalance, and not bearing faults. ISO vibration limits are inches/second, were the conversion from inches to G's is. $G = 0.0162 * V * f$. In general, 1 inch/sec is considered damaging vibration levels.

Many software packages output spectrum in power (G^2/Hz), but prior research (Bechhoefer 2008) revealed that the correlation between damage and energy (G's) was linear. For this reason, the units are in G's.

2. SYNCHRONOUS RESAMPLING

The model for vibration in a shaft in a gear box was given in (McFadden 1987) as:

$$x(t) = \sum_{i=1:K} X_i(1 + a_i(t))\cos(2\pi i f_m(t) + \Phi_i) + b(t) \quad (1)$$

where:

- X_i is the amplitude of the k th mesh harmonic
- $f_m(t)$ is the average mesh frequency
- $a_i(t)$ is the amplitude modulation function of the i th feature harmonic.
- $\phi_i(t)$ is the phase modulation function of the i th feature harmonic.
- Φ_i is the initial phase of harmonic k , and
- $b(t)$ is additive background noise.

The mesh frequency is a function of the shaft rotational speed: $f_m = Nf(t)$, where N is the number of teeth on the gear and $f(t)$ is the shaft speed as a function of time. For bearings, N is the component rate, which is a non-integer value based on the bearing geometry. As noted, because of the finite bandwidth of the feedback control, or due to the environment, there is some wander in the shaft speed. This change in speed will result in smearing of amplitude energy in the frequency domain.

If a tachometer signal is present (such as a key phasor) and the ratio from the key phasor to the shaft under analysis, the vibration data can be resampled such that number of data points between one revolution and the next is the same. In the case of time synchronous averaging (TSA), the ensemble average of EQ(1) is calculated summing each

revolution of resampled data, then dividing by the number of revolutions during the acquisition. .

Since the radix-2 FFT is most commonly used, the number of data points in one shaft revolution (r_n) are interpolated into m number of data points, such that:

- For all shaft revolutions n , m is larger than r , and
- $m = 2^{\text{ceiling}(\log_2(r))}$ (again assuming Radix 2 DFT)

Since some other analysis process will be done on the resampled signal (envelop analysis, for example) – a radix-2 length is not necessary. However, for this example a Radix 2 length was used to calculate the resample length m . The algorithm resamples index r_i in m data points, the concatenates them into a new vector. Once all of the data is resampled, the envelope/spectrum is taken. Figure 3 compares the TSA algorithm to the Resampling algorithm.

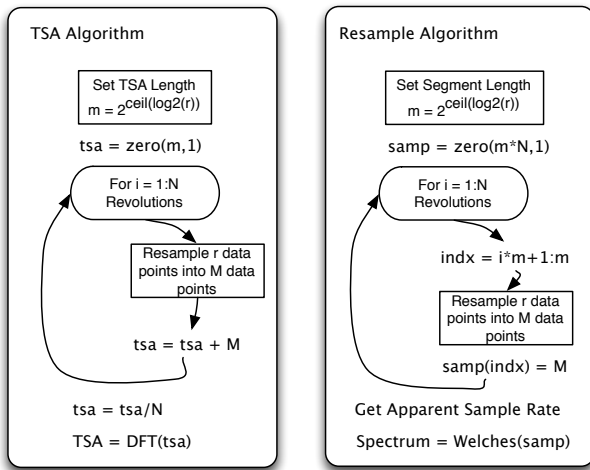


Figure 3 TSA and Resample Algorithm Flow

2.1. Example: Synchronous Resampling Algorithm

For example, say the sample rate was 1000 samples per second, and the lowest shaft rate was 10 Hz, for a .5 second acquisitions. The resample length, m , is 128. The number of data points between each key phasor is: 87, 92, 100, 95, 89, 37. For each shaft revolution, the data is resampled to length l : Rev 1: 87->128, Rev 2: 92->128, Rev 3: 100->128, Rev 4: 95->128, Rev 5: 89->128. Note that for half of a second of data, there is 640 data points – the remaining 37 data were in the next, incomplete revolution, so the last 37 data points are dropped. The resample length is taken at the next largest power of 2 over the maximum length of all revolutions, again, assuming a radix 2 DFT.

Because of interpolation, the sample rate for each revolution is now changed. To accurately determine the frequency associated with a DFT bin, an apparent sample rate is needed. The apparent sample rate is the original sample rate

* length of the resampled data / length of the original data: $1000 * 640 / (463)$, or 1382.

2.2. TSA for Bearing Analysis

For shaft and gear analysis, existing TSA algorithms control for changes in shaft speed. For bearing, because they do not have integer number of shaft for a rate, the TSA is felt to be inappropriate for three reasons:

- Bearings are quasi-stationary – there is always some slippage such that even with correct geometry, the rates are not exact. This will make the bearing component non-synchronous with the TSA algorithm and in fact may separate the bearing signal out of the TSA.
- A bearing has rates for each component: cage, ball, inner and outer race. This would require the TSA to be run four separate times for each bearing, in order to capture the energy for each bearing component. While this may not be a problem for off line analysis, it may exceed the resources of an on-line analysis system. Considering that any given shaft is supported by 2 to 3 bearings, which would require 8 to 12 TSA analyses.
- In the evaluation of bearing health, it is important to be able to observe the relationship between the shaft, cage, ball, inner and outer race fault features. For example, an inner race fault that is modulated by shaft (e.g. side bands that are 1 shaft rate off of the inner race fault) is a more serious fault than an inner race fault, as it indicates wear and clearance issues on the shaft. The ability to view modulation between bearing components and shaft is a powerful diagnostics tool that is not available if using the TSA for each bearing components

That said, the structure of the TSA is the model for which this resample algorithm is based.

3. HIGH SPEED SHAFT BEARING FAULT

A commercial wind turbine with a 2 MW power output was installed with a condition monitoring system. Data was collected at 10-minute intervals. The data was sampled at 97656 sps for 6 seconds. Bearing envelop analysis was performed by band passing the signal between 9 to 11 KHz. Welches spectrum was used on the heterodyned signal with a DFT length of 4096, and with an overlap of 2048 points. Increased inner race energy on the high-speed shaft bearing indicated a fault (Figure 2). An inspection of the bearing latter showed that the inner race was cracked. Using this data, the raw spectrum was compared to the resampled spectrum and the TSA (Figure 4). The spectrum length was

the same as the TSA length, so that the plots have similar bin widths.

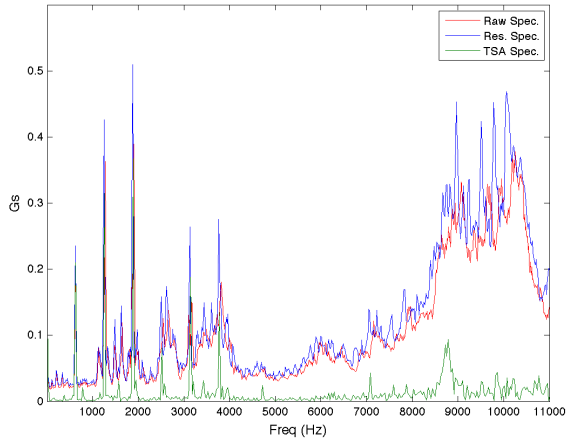


Figure 4. Raw, resampled, and TSA spectrum

The average shaft rate is 30.9 Hz. This shaft is driven by a 20-tooth pinion. The first 6 harmonics of the pinion are clearly visible at 620, 1240, 1860, 2480, 3100 and 3720 Hz. The TSA ran 188 revolutions, so that the noise floor of the TSA is approximately $1/\sqrt{188}$, or $0.073x$ that of the raw or resampled spectrums (Bechhoefer, 2009).

In Figure 5, a detailed view of the spectrum is given from 2200 to 4000 Hz, showing that the resampled spectrum has more spectral content than the raw spectrum or the TSA spectrum. In the 9000 to 10,500 Hz view, spectral peaks are visible 9220, 9510 9800 and 10,090 Hz.

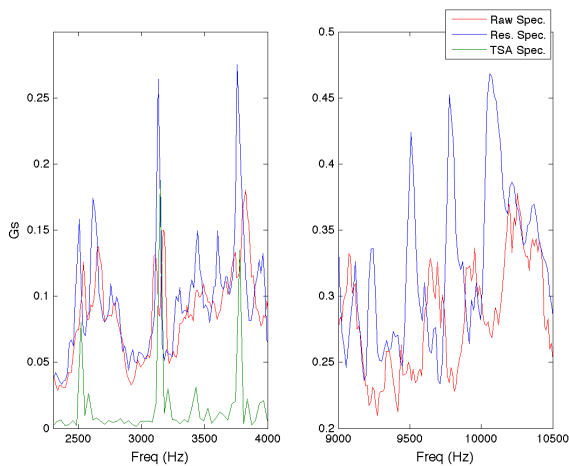


Figure 5. Detail of raw, resampled and TSA spectrum

The 290 Hz difference is close to the modulation rate of an inner race fault, which was 292 Hz. The high, broadband spectrum is indicative of bearing resonance. Because resonance is non-synchronous, the TSA does not capture this bearing resonance.

As an aside, plotting the TSA against the raw spectrum is a good way to identify bearing faults: Frequency content not present in the TSA which are present in the raw spectrum can only be gear mesh frequencies from other shafts in the gearbox, or a bearing fault.

The envelope of the raw and resampled data was taken with a window from 9KHz to 11KHz. This “window” covers the spectrum where bearing resonance is present. This is essential for successful bearing analysis using the envelope technique (Bechhoefer, 2010), see Figure 4. The raw and resampled envelope spectrum is seen in Figure 6.

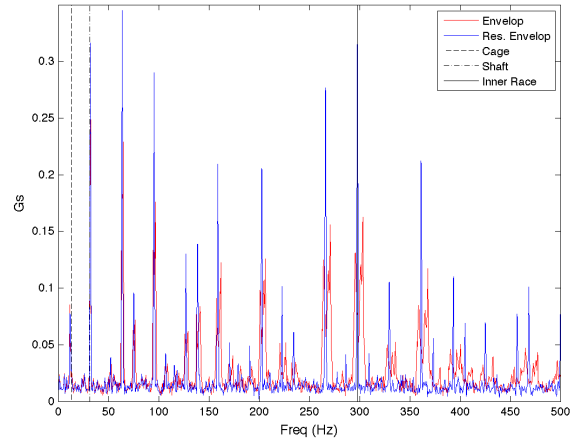


Figure 6. Envelope spectrum of raw and resampled data

Note that the cage (13 Hz), shaft (31 Hz) and inner race fault feature (292 Hz) are overlaid on the spectrum. Clearly, the resampled envelope spectrum fault features have greater energy. This is not a scale issue, as the noise floor for both spectrums are the same. The increased energy is because there is less spreading of energy into neighboring FFT bins. Figure 7 gives a detail view of the spectrum.

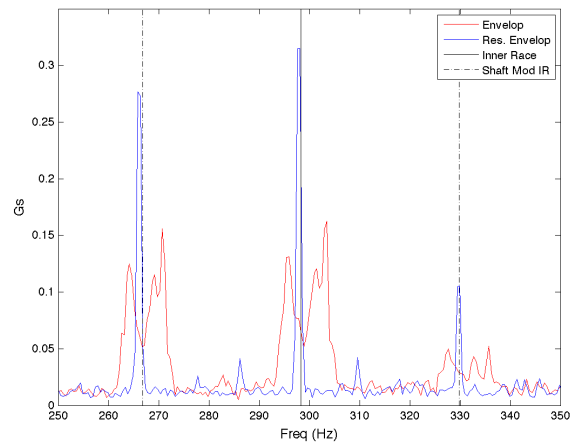


Figure 7. Detail view of inner race fault: envelope spectrum

This view highlights the improvement in resolution of the resampled data over the raw data. Note that from Table 1,

the fault frequency range for the inner race was 292 to 303 Hz, which is validated in Figure 7 in the raw envelope spectrum. Note that maximum value of the raw envelope spectrum was 0.17 Gs. As seen in the resampled spectrum, the true energy value is closer to .32 G's or a 47% error in the original measurement. This smearing of measurement data, results in additional noise in the CI measurement (Figure 2). This noise in the measured CI is caused by the large variance in shaft speed.

Both inner race modulated by cage and inner race modulated by shaft are also clearly present in the resampled envelope spectrum. This type of information gives a maintainer additional diagnostics, which are missing in the raw spectrum.

3.1. Testing The Hypothesis on Shaft Speed as a Source of Variance

It is hypothesized that at least some of the variance in trend of the inner race energy was due to non-constant shaft speed. As previously noted, it was shown variation in shaft speed smears the measured energy associated with a fault in the spectrum. A test of this hypothesis could be done if one could reprocess the vibration data in Figure 2. Unfortunately, raw data is collected only once per day (1 out of 144 acquisitions). This subset or raw data was reprocessed using and the measured inner race energy was calculated for the raw envelop spectrum, and the resampled envelop spectrum, over 50 days, and compared in Figure 8.

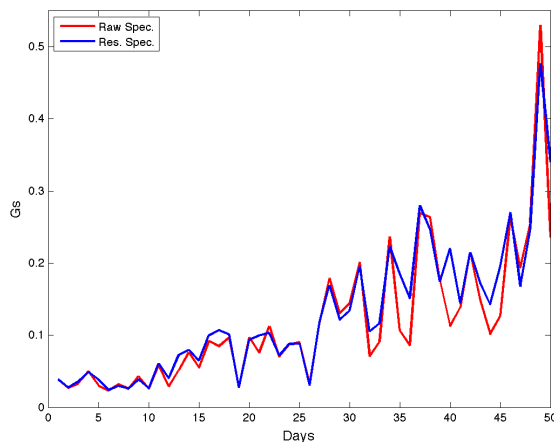


Figure 8. Raw and resampled inner race envelope energy over 50 days

It is easily observed that the resampled envelope energy is higher than the raw envelop. This would be expected in that, because there is less smearing of energy, there is more energy associated with the fault. To formally test this hypothesis: H_0 That resampling does not change the CI variance, vs. H_A That the resampling reduces the CI variance.

The sample variance was calculated from the de-trended data from day 25 to day 48. The sample variance for the raw envelop spectrum was 0.0047 ($\sigma = 0.068$), while for the resampled envelope, the variance was 0.002, ($\sigma = 0.045$), with an F statistic of 2.3 (approximately 57% reduction in variance). This is significant an alpha of 0.05 and 22 degrees of freedom, reject the null hypothesis that resample does not effect CI variance.

4. CONCLUSION

Condition monitoring of rotating machinery is complicated by the fact that machines under analysis do not always run at a constant rate. While the time synchronous average can be used to control variance in machine speed for shafts and gears – there is not such standard practice or algorithm to control variance in shaft speed for bearing or other non-synchronous analysis.

In general, it is assumed that the effect of spectral smearing due to variance in shaft speed is small. However, variation in shaft speed is commonly observed in the field. This problem is especially great for wind turbines, in which there is variation due to: changing wind speed, a 3/revolution torque ripple due to tower shadow, and a 1/revolution effect from wind shear. It is not surprising to see a 4% change in shaft speed in a 6 second acquisition.

In this paper, a resampling algorithm was developed in which raw data is synchronized by a key phasor to a shaft under analysis. The resampling process changes the effective sample rate and normalizes the data by removing the effect of changes in shaft speed. It allows both synchronous (shaft/gear) analysis and non-synchronous (bearing, bearing resonance) analysis.

This is demonstrated on a wind turbine high speed shaft bearing with an inner race fault. It is shown that by resampling, the frequency content of the envelop spectrum, which is spread over a frequency of 292 to 303 Hz (14 FFT bin), with raw envelope spectrum of 0.17 Gs. For the resampled spectrum, the true energy value is closer to .32 Gs. For this example, the raw energy spectrum had an error of 47% when compared to the resampled spectrum.

The hypothesis was tested that the resampled envelope energy for a fault would have lower variance. This was tested by reprocessing vibration data for a known fault with 50 samples. The reduction in variance was statistically significant at alpha of .05, or approximately a 55% reduction in variance.

This is a significant improvement in performance. This indicates that variation in speed accounts for a large variance in condition indicator values. Fielding this improved analysis algorithm will result in:

- Bearing faults will be easier to identify,

- That threshold setting will be simplified,
- That trend analysis will be improved and finally,
- That this will facilitate an improved prognostics capability.

The resampling algorithm used linear interpolation, but spline or cubic interpolation could be used.

REFERENCES

- ISO 10816 Vibration Severity Standards.
- Bechhoefer, E., He, D., (Bechhoefer 2008), Bearing Prognostics using HUMS Condition Indicators, American Helicopter Society 64th Annual fourm, Montreal.
- McFadden, P., Smith, J., (McFadden 1985), A Signal Processing Technique for detecting local defects in a gear from a signal average of the vibration. Proc Instn Mech Engrs.
- McFadden, P., (McFadden 1987) "A revised model for the extraction of periodic waveforms by time domain averaging", Mechanical Systems and Signal Processing 1 (1) 1987, pages 83-95
- Bechhoefer, E., Kingsley, M. (Bechhoefer 2009a). "A Review of Time Synchronous Average Algorithms". Annual Conference of the Prognostics and Health Management Society
- Christian, K., Mureithi, N, Lakis, A., Thomas, M., (Christian, 2007), "On the use of Time Synchronous Averaging, Independent Component Analysis and Support Vector Machines for Bearing Fault Diagnosis", First International Conference on Industrial Risk Engineering, Montreal, Dec 17-19 Montreal.
- Bechhoefer, E., Kingsley, M., Menon, P., (Bechhoefer, 2009b), "Bearing Envelope Analysis Window Selection Using Spectral Kurtosis Techniques", IEEE PHM Conference, 2011.

BIOGRAPHIES

Eric Bechhoefer received his B.S. in Biology from the University of Michigan, his M.S. in Operations Research from the Naval Postgraduate School, and a Ph.D. in General Engineering from Kennedy Western University. His is a former Naval Aviator who has worked extensively on condition based maintenance, rotor track and balance, vibration analysis of rotating machinery and fault detection in electronic systems. Dr. Bechhoefer is a board member of the Prognostics Health Management Society, and a member of the IEEE Reliability Society. Dr. Bechhoefer is partner and President of Green Power Monitoring Systems, LLC, which is a developer of condition monitoring equipment for remote monitoring.

Brandon Van Hecke received his B.S. in Industrial Engineering from the University of Illinois at Chicago in 2010. He is a Ph.D. candidate in the Department of Mechanical and Industrial Engineering. His research interests include digital signal processing, machinery health monitoring and fault diagnostics based on the evaluation of vibration and acoustic emission signals, and condition based maintenance.

David He received his B.S. degree in metallurgical engineering from Shanghai University of Technology, China, MBA degree from The University of Northern Iowa, and Ph.D. degree in industrial engineering from The University of Iowa in 1994. Dr. He is a Professor and Director of the Intelligent Systems Modeling & Development Laboratory in the Department of Mechanical and Industrial Engineering at The University of Illinois-Chicago. Dr. He's research areas include: machinery health monitoring, diagnosis and prognosis, complex systems failure analysis, quality and reliability engineering, and manufacturing systems design, modeling, scheduling and planning.